Presented at the 6th Annual CMAS Conference, Chapel Hill, NC, October 1-3, 2007

DIAGNOSTIC AND MECHANISTIC EVALUATIONS OF MM5-CMAQV4.6 FOR THE SUMMER 2000 CENTRAL CALIFORNIA OZONE STUDY

Ling Jin, Nancy J. Brown*, Shaheen Tonse
Atmospheric Science Department, Lawrence Berkeley National Laboratory, Berkeley, CA, USA

Robert A. Harley,
Department of Civil and Environmental Engineering, University of California , Berkeley, CA, USA

Jian-wen Bao, Sara A. Michelson, and James Wilczak
Regional Weather and Climate Applications Division NOAA/Environmental Technology Laboratory, 325 Broadway, Mail Stop: ET7, Boulder, CO, USA

1. INTRODUCTION

Past evaluations of Community Multiscale Air Quality (CMAQ) (Byun, 2006) modeling system have focused on the eastern United States and applications of it are usually conducted for high ozone episodes that last for a few days. In our research, we seek more comprehensive model evaluation by applying MM5-CMAQ to simulating ozone formation for an entire summer season in central California, where ozone air pollution problems are severe and air districts are out of compliance with the 8-hour ozone standard.

In this study, we apply the Community Multi-Scale Air Quality model (CMAQ version 4.6) to a 15-day period contained in the summer 2000 Central California Ozone Study. Model parameters and inputs are set to reflect actual conditions of the modeling domain. We apply a variety of evaluation and diagnostic methods to assess model performance across a range of days and locations, with significant spatial and temporal variations in air quality. Effects of meteorological data assimilation are evaluated. We perform sensitivity analyses with the brute force method and Direct Decoupled method (DDM) (Dunker, 1984, 2002) to diagnose causes for discrepancies between observations and model predictions.

2. METHODS

2.1 Modeling Domain

The San Joaquin Valley is surrounded by Sierra Nevada and coastal mountain ranges. On typical summer days, westerly winds are funneled into the Central valley through gaps in the coastal range with large portions of the flow directed into the San Joaquin valley. The San Francisco Bay area and Sacramento valley are the major upwind emission sources affecting air quality in the San Joaquin valley. The study domain is gridded into 96 by 117 cells, with a horizontal resolution of 4 km. Vertically, the domain is divided into 27 layers from the surface to 100 mb (about 17 km); the near surface layers are about 20 m thick.

2.2 Emission Inputs

Model inputs were developed that describe variability in atmospheric conditions, including day-specific emission rates from both natural and anthropogenic sources. Anthropogenic emissions from area, and point sources were derived from the gridded emission inventory data provided by the California Air Resources Board. Motor vehicle emission inventory estimates describe light-duty gasoline and heavy-duty diesel vehicle activity patterns and emissions separately by time of day and day of week using the methodology developed by Harley et al. (2005). Biogenic VOC emissions (mainly isoprenes and terpenes) were estimated hourly with the BEIGIS modeling system (Scott and Benjamin, 2003, Steiner et al., 2006).

2.3 Meteorology Inputs

Gridded hourly meteorological fields were developed using the MM5 meteorological model (Grell, 1994) for the 15 day period from July 24 to August 8, 2000, using three nested grids: an outer 36 km resolution grid, within which is nested a 12 km grid, within which is nested the 4 km CCOS grid with 190 cells in each horizontal direction and 50 vertical layers. The 4 km resolution MM5 output is used to drive CMAQv4.6 simulation.

**Corresponding author:* Nancy J. Brown, Atmospheric Science Department, Lawrence Berkeley National Laboratory, Berkeley, CA 94720; e-mail: njbrown@lbl.gov.

The middle 5-day period (a high ozone episode) is characterized by an offshore pressure gradient caused by a large high-pressure system over Utah and Colorado, with reduced incoming westerly flow at the coast and stagnate conditions in the valley. Four dimensional data assimilation was conducted for this 5-day ozone episode using data from a network of surface wind observations, and radar wind profilers.

2.4 Boundary Conditions and Parameter Adjustments

Constant pollutant concentrations are set for each of the four lateral boundaries of the domain. The western inflow boundary is mostly over the ocean and its chemical species concentrations are set to clean marine background values. Vertically varying O_3 is based on averaged August ozone sonde measurements made at Trinidad Head, CA (Newchurch, 2003). Nitrogenous species (NO: 0.01 ppb; NO2: 0.03 ppb; etc.) and a suite of VOC species take values measured in the marine background free troposphere (Nowak, 2004). The other three boundaries are dominated by outflows; the same boundary values used in past studies conducted in this domain by the California Air Resources Board (Kaduwela, 2006, personal communication) are used here.

Ozone dry deposition velocity over the ocean is increased from the CMAQ default value of zero to 0.04 cm/s according to measured values (Faloona, 2006, personal communication). Minimum eddy diffusivity (Kzmin) in CMAQ default value (0.5 m/sec^2) appears too high for stable marine layers on the western boundary, and this causes excessive vertical mixing and increases surface ozone. Assuming wind speeds of about 10 m/s and surface roughness lengths for the ocean to be between the suggested values of 1.5×10-5 and 1.5×10-3 m, we calculated Kz to be between 0.0015 and 0.15 m/sec^2. Kzmin is thus set to 0.1 m/sec^2.

2.5 Evaluation and Diagnostic Tools

Different evaluation methods address model performance from various perspectives. The evaluation methods employed in this study are summarized in the following table.

Sensitivity analysis with the brute force method and Direct Decoupled method (DDM) (Hakami, 2003) are used to diagnose causes for discrepancies between observations and model predictions.

Table 1 Summary of evaluation methods.

Methods	**Usage**
Taylor's Diagram	Describe how well patterns in modeled and observed values match each other
Mean Bias	Average sign in model prediction errors
RMSE, Gross Error	Magnitude of model prediction errors
Spatial Krigging	Spatial variation in model performance
Ozone Production Efficiency	Limiting regimes presented in the observed and modeled air masses

3. MODEL SIMULATION AND EVALUATION

Our 15-day simulation is driven by the prognostic meteorology in CMAQv4.6, configured with SAPRC99 (Carter, 2000) chemical mechanism. Additional simulations for the middle 5-day ozone episode are performed using nudged meteorological fields. Highest ozone levels occur on Aug 1st and 2nd (Julian days 214 and 215).

3.1 Spatial and Temporal Trends in Model Performance

The model's ability to reproduce the variation and correct levels of observed ozone is examined with a Taylor diagram (Taylor, 2001) and normalized biases. We report daytime comparison statistics with respect to ozone. At night, when strong convective mixing is absent, observed ozone at measurement sites are often more affected by titration with NO emitted at nearby roadways. Hence we compare odd oxygen O_x (NO_2+O_3) concentrations to evaluate model performance at night.

On a Taylor diagram the correlation coefficient and the root-mean-square difference (RMSD) between the modeled and observed values, along with the ratio of the standard deviations of the two patterns are all indicated by a single point on a two-dimensional plot (Fig. 1). Across the three air basins that have the highest ozone levels, model simulation of the middle 5-day ozone episode shows a consistent better match to the observed standard deviation, while the first 5-day period shows consistent better linear correlations and root mean squared differences across the three air basins. In general, points representing modeled patterns in different air basins and time periods are clustered together, indicating a similar model performance across time and space. All the pattern metrics indicate that model performance in the San Francisco Bay area during the last 5-day period needs improvements relative to the first two 5-day periods.

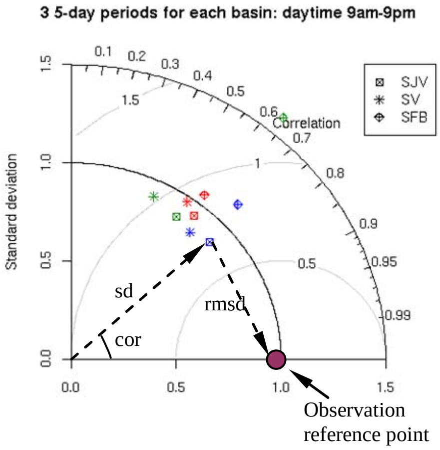

Fig. 1. Taylor diagram showing daytime evaluation statistics normalized by observed standard deviation, for July 24-29 (blue), July 29-August 2 (red), August 2-7 (green), respectively, at three air basins: the San Joaquin Valley (SJV), the Sacramento Valley (SV), and the San Francisco Bay area (SFB).

Pattern statistics are useful for comparing the anomalies in two data sets, while normalized mean bias indicates either over-prediction or under-prediction. From Fig. 2 we see that the model slightly under-predicts daytime ozone in the San Joaquin Valley and Sacramento Valley in general, but over-predicts ozone in the Bay area, especially for the first half of the simulation period. There is no clear temporal trend in model biases, but we do observe over-prediction on the last day, and this corresponds to the positive bias present in MM5 temperature fields during that day.

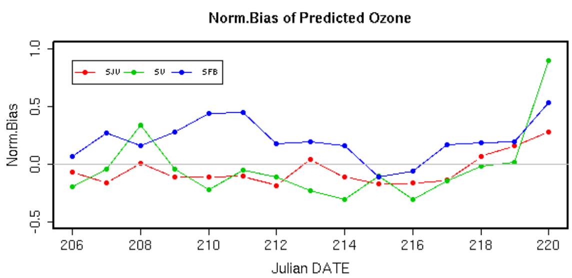

Fig. 2. Daytime normalized biases at three air basins with cutoff value of 10 ppb.

Table 2 shows evaluation metrics for modeled peak ozone, daytime NO_x, and nighttime O_x across the three 5-day periods. Gross errors suggest CMAQ does a better job in predicting peak ozone concentrations than the precursor concentrations. There is a slight improvement in peak ozone prediction over three 5-day periods, as suggested in the normalized biases. Overall, CMAQ under-predict peak ozone concentrations.

Table 2 Summary statistics for three 5-day period.

	Normalized Bias			Normalized Gross Error		
	1	2	3	1	2	3
1h Peak O_3	-10%	-7%	-4%	17%	20%	18%
8h Peak O_3	-15%	-12%	-11%	17%	17%	18%
Daytime NO_x	0%	-4%	3%	57%	60%	64%
nighttime O_x	8%	10%	8%	19%	29%	22%

Peak ozone cutoff value: 60 ppb, NO_x and O_x: 10 ppb.

3.2 Effects of Meteorology Nudging on Air Quality Simulations

Four dimensional data assimilation provides clear improvements in MM5 simulated wind fields (Fig. 3, 4), in terms of wind speed and direction at all altitudes presented here. The largest improvements appear on Day 214, when we also see the largest improvements in spatial ozone biases (Fig. 5).

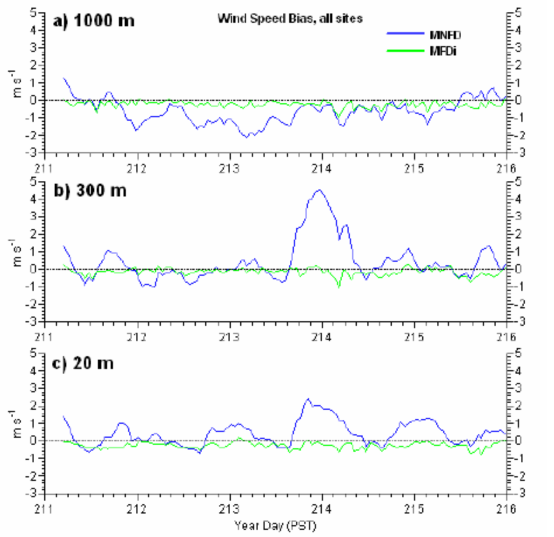

Fig. 3. Domain averaged wind speed biases with (MFDi) and without (MNFD) four dimensional data assimilation.

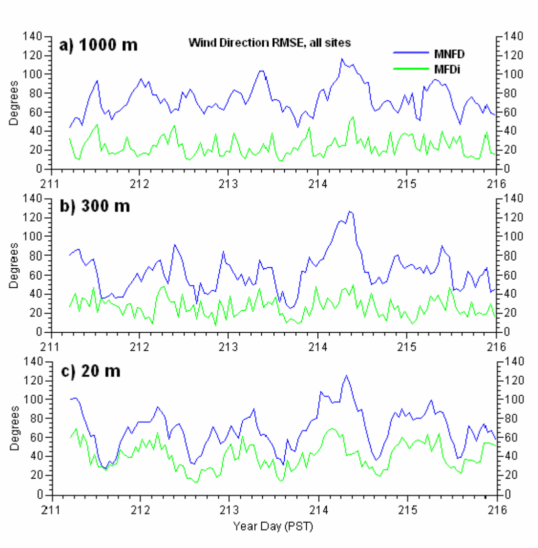

Fig. 4. Domain averaged wind direction biases with (MFDi) and without (MNFD) four dimensional data assimilation.

Improved wind speed and direction ensure better representation of chemical transport in the model, which leads to more correct localization of ozone plumes. Ozone biases on Day 214 are krigged (Cressie, 1993) to generate a continuous error surface and are shown at 3 PM local time, when ozone levels are the highest. Before wind nudging, modeled meteorology appears to have less strong westerly flows, which prevents the Bay area ozone plume from entering the San Joaquin valley, and causes excessive over prediction in the Bay area and under prediction in the northern San Joaquin valley. Another significant improvement occurs in the Sacramento valley. Before nudging, the southward winds appear to be too strong in the Sacramento valley, resulting a shorter residence time for local pollutants to build up. Thus we observe a large under-prediction of ozone in Sacramento. After observational nudging, ozone biases are reduced by about factor of two.

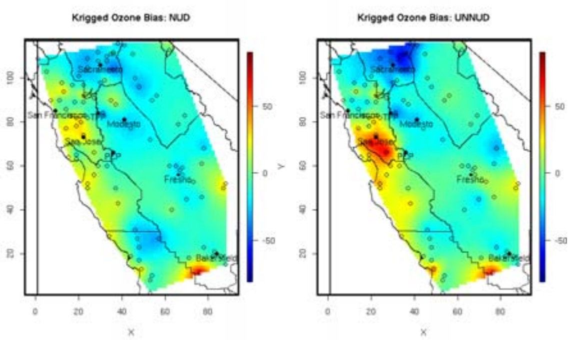

Fig. 5. Predicted ozone biases on Day214 at 3 pm PDT with (NUD) and without (UNNUD) nudged wind.

3.3 Ozone Production Efficiency

Up to now we have only examined model performance in terms of predicting individual species concentrations. Previous study related odd oxygen O_x to NO_z in terms of ozone production efficiency (OPE) (Trainer et al., 1993), which is defined here as the slope when we plot O_x against NO_z (Mena-Carrasco et al. 2007). Ozone production efficiency reflects ozone sensitivity to NO_x in the air mass of interest, and thus can be used to evaluate how well modeled ozone sensitivities match the observed ones. Sources of discrepancy between modeled and observed OPE at a particular location and time include incorrect mixtures of emission inputs, insufficient representation of ozone chemistry, and misplacement of ozone plumes by transport errors. We present weekday OPEs in the middle 5-day period, at three sites where the daytime NO_z observations are available (Fig. 6). Fortunately, ozone chemistry at these sites represents three typical air masses in terms of their distances from the major nearby emission sources. Turlock station is located in northern San Joaquin Valley, far downwind of Bay area emissions, and often experiences aged air masses (NO_x poor) transported from the Bay area. Fresno is right at the urban emission center in the middle San Joaquin valley, representing air masses of fresh emissions rich in NO_x. Arvin station in the southern San Joaquin Valley is in the intermediate downwind of Bakersfield emissions. OPE is considered separately for modeled data driven by meteorology with and without four dimensional data assimilation to investigate the effects of transport errors on predicted OPEs. In Fig 6, we see modeled OPEs with or without wind nudging are both very close to observed ones at Turlock and Fresno stations. A large OPE at Turlock station indicates efficient ozone production, typical of NO_x-limiting conditions in aged air masses. OPE at Fresno station is much lower, which reflects the fact that the air mass is very close to the emission sources. Observed OPE (6.1) at Arvin station indicates NO_x-limiting conditions, while modeled OPE (3.3) without wind nudging implies less aged air masses sampled at this station. Wind nudging brings modeled OPE from 3.3 to 5.3, much closer to the observed value. As the first two stations are either far away from or very close to the emission sources, ozone sensitivities to NO_x in the air masses there are both less affected by transport errors. In contrast, wind direction and speed determine how much Arvin station is influenced by its nearby upwind emissions in Bakersfield. We see similar modeled and observed OPEs across all three sites when nudged wind fields are used, indicating adequate representation of ozone sensitivities in the model.

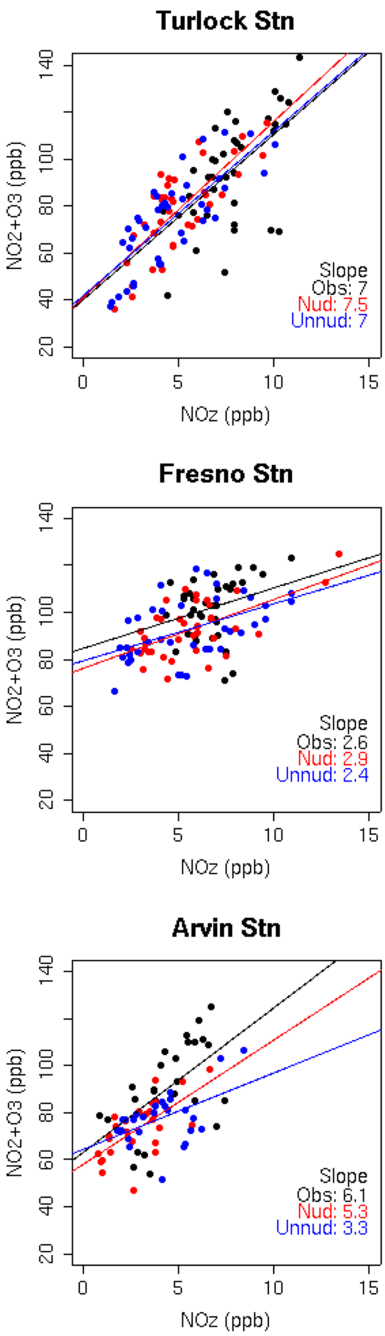

Fig. 6. Ozone production efficiency (the linearly fitted slope) at three sites evaluated for observed and modeled daytime data during weekdays in the middle 5-day period.

3.4 Sensitivity Analysis

We have seen that CMAQ generally over predicts ozone on the west coast, but under-predicts ozone in the central valley. Sensitivity analyses with brute force and decoupled direct methods are employed to determine the most influential factors of simulated ozone concentrations at various geographical locations. We evaluate ozone sensitivities to a number of input parameters: boundary conditions (ozone, volatile organic compounds (VOC), nitrogen oxides), boundary ozone at different heights, emissions of NO_x, anthropogenic VOCs (AVOC), and biogenic VOCs (BVOC). We found that the coastal areas are most sensitive to NO_x emissions and boundary ozone conditions, especially those at the surface level. The San Francisco Bay area is sensitive to both anthropogenic and biogenic emissions, as well as boundary conditions, while central valley is more sensitive to anthropogenic emissions.

4. CONCLUSIONS

In this paper, we have simulated ozone formation in the central California region with CMAQv4.6 for a 15-day period, which includes a five-day high ozone episode. We have applied a number of evaluation methods to assess model performances. Simulated ozone concentrations adequately match the observed pattern, except in the Bay area during the last 5-day period. Model performance does not degrade over time, but exhibits spatial trends in biases. CMAQ tends to over-predict ozone at coastal areas, and slightly under-predict in the central valley. Wind nudging greatly improves the chemical transport processes. When transport errors are minimized, we see similar ozone sensitivities when comparing observed and modeled ozone production efficiencies. Sensitivity analysis is performed and the most influential factors studied here are listed for different geographical regions. The Bay area is sensitive to uncertainties in all the input parameters considered here, which suggests great challenges on correct simulating ozone concentrations in this area.

5. ACKNOWLEDGMENTS

Support for this study was provided by the California Energy Commission, the California Air Resources Board, the UC Toxic Substances Research and Teaching Program Student

Fellowship, and by the Assistant Secretary for Fossil Energy, Office of Natural Gas and Petroleum Technology through the National Petroleum Technology Office under U.S. Department of Energy Contract No. DE-AC03-76SF00098. The authors thank Allison Steiner for providing the biogenic emission inventory used in this research.

6. REFERENCES

Byun, D. W.; Schere, K. L. Review of the governing equations, computational algorithms, and other components of the Models-3 Community Multiscale Air Quality (CMAQ) modeling system. *Applied Mechanics Reviews*. **2006**, Vol. 59, No. 2, p. 51-77.

Carter, W. P. L. Implementation of the SAPRC-99 Chemical Mechanism into the Models-3 Framework. University of California, Riverside, California. Report to the U.S. Environmental Protection Agency, Washington, D. C., **2000**.

Cressie, N.A.C. Statistics for Spatial Data, Wiley, New York,**1993** (revised edition) .

Dunker, A.M. The decoupled direct method for calculating sensitivity coefficients in chemical kinetics, *J. Chem. Phys.* **1984**, *81*, 2385-2393.

Dunker, A.M.; Yarwood, G.; Ortmann, J. P.; Wilson, G. M. The decoupled direct method for sensitivity analysis in a three-dimensional air quality model: Implementation, accuracy, and efficiency, *Environ. Sci. Technol.* **2002**, *36* (13), 2965 -2976.

Grell, G.A.; Dudhia, J.; Stauffer, D. R. A description of the fifth-generation Penn State/NCAR mesoscale model (MM5). NCAR Technical Note, NCAR/TN-398+STR, 122 pp., NCAR, Boulder, CO, **1994**.

Hakami, A.; Odman, M. T.; Russell, A. G. High-order, direct sensitivity analysis of multi-dimensional air quality models, *Environ. Sci. Technol.* **2003**, *37* (11), 2442-2452.

Harley, R.A.; Marr, L. C.; Lehner, J. K.; Giddings, S. N. Changes in motor vehicle emissions on diurnal to decadal time scales and effects on atmospheric composition, *Environ. Sci. and Technol.*, **2005**, 39, 5356-5362.

Mena-Carrasco, M.; Tang, Y.; Carmichael, G. R.; Chai, T.; Thongbongchoo, N.; Campbell, J. E.; Kulkarni, S.; Horowitz, L.; Vukovich, J.; Avery, M.; Brune, W.; Dibb, J. E.; Emmons, L.; Flocke, F.; Sachse, G. W.; Tan, D.; Shetter, R.; Talbot, R. W.; Streets, D. G.; Frost, G.; Blake, Donald. Improving regional ozone modeling through systematic evaluation of errors using the aircraft observations during the International Consortium for Atmospheric Research on Transport and Transformation. *J of Geophys. Res.* **2007**, Vol 112, D12S19, doi: 10.1029/2006JD007762.

Newchurch, M. J.; Ayoub, M. A.; Oltmans, S.; Johnson, B.; Schmidlin, F. J. Vertical distribution of ozone at four sites in the United States. *J. Geophys. Res.* **2003**, 108, D14031: doi: 10.1029/2002JD002059.

Scott, K. I.; Benjamin, M. T. Development of a biogenic volatile organic compound emission inventory for the SCOS97-NARSTO domain, *Atmos. Environ.*, **2003**, 37(2), S39-S49.

Steiner, A. L.; Tonse, S.; Cohen, R. C.; Goldstein, A. H.; Harley, R. A. Influence of future climate and emissions on regional air quality in California, *J. Geophys. Res.*, **2006**, 111, D18303, doi:10.1029/2005JD006935

Taylor, K.E. Summarizing multiple aspects of model performance in a single diagram. *J. of Geophys. Res*. **2001**, *106*(D7), 7183–7192.

Trainer, M.; Parrish, D. D.; Buhr, M. P.; Norton, R. B.; Fehsenfeld, F. C.; Anlauf, K. G.; Bottenheim, J. W.; Tang, Y. Z.; Wiebe, H. A.; Roberts, J. M.; Tanner, R. L.; Newman, L.; Bowersox, V. C.; Meagher, J. F.; Olszyna, K. J.; Rodgers, M. O.; Wang, T.; Berresheim, H.; Roychowdhury, U. K. Correlation of ozone with NO_y in photochemically aged air, *J. Geophys. Res.* **1993**, 98, 2917-2925.